Received: 28 November 2023 | Revised: 2 April 2024 | Accepted: 5 April 2024

DOI: 10.1002/biot.202300664

Biotechnology Journal

RESEARCH ARTICLE

CYP116B5-SOX: An artificial peroxygenase for drug metabolites production and bioremediation

Daniele Giuriato | **Gianluca Catucci** | **Danilo Correddu** | **Giovanna Di Nardo** | **Gianfranco Gilardi**

Department of Life Sciences and Systems Biology, University of Torino, Torino, Italy

Correspondence
Gianfranco Gilardi, Department of Life Sciences and Systems Biology, University of Torino, Via Accademia Albertina 13, 10123, Torino, Italy.
Email: gianfranco.gilardi@unito.it

Abstract

CYP116B5 is a class VII P450 in which the heme domain is linked to a FMN and 2Fe2S-binding reductase. Our laboratory has proved that the CYP116B5 heme domain (CYP116B5-hd) is capable of catalyzing the oxidation of substrates using H_2O_2. Recently, the *Molecular Lego* approach was applied to join the heme domain of CYP116B5 to sarcosine oxidase (SOX), which provides H_2O_2 in-situ by the sarcosine oxidation. In this work, the chimeric self-sufficient fusion enzyme CYP116B5-SOX was heterologously expressed, purified, and characterized for its functionality by absorbance and fluorescence spectroscopy. Differential scanning calorimetry (DSC) experiments revealed a T_M of 48.4 ± 0.04 and 58.3 ± 0.02°C and a enthalpy value of 175,500 ± 1850 and 120,500 ± 1350 cal mol^{-1} for the CYP116B5 and SOX domains respectively. The fusion enzyme showed an outstanding chemical stability in presence of up to 200 mM sarcosine or 5 mM H_2O_2 (4.4 ± 0.8 and 11.0 ± 2.6% heme leakage respectively). Thanks to the in-situ H_2O_2 generation, an improved k_{cat}/K_M for the *p*-nitrophenol conversion was observed (k_{cat} of 20.1 ± 0.6 min^{-1} and K_M of 0.23 ± 0.03 mM), corresponding to 4 times the k_{cat}/K_M of the CYP116B5-hd. The aim of this work is the development of an engineered biocatalyst to be exploited in bioremediation. In order to tackle this challenge, an *E. coli* strain expressing CYP116B5-SOX was employed to exploit this biocatalyst for the oxidation of the wastewater contaminating-drug tamoxifen. Data show a 12-fold increase in tamoxifen *N*-oxide production—herein detected for the first time as CYP116B5 metabolite—compared to the direct H_2O_2 supply, equal to the 25% of the total drug conversion.

KEYWORDS
cytochrome P450, environmental pollution, H_2O_2 in-situ generation, molecular Lego, protein engineering

1 | INTRODUCTION

The persistence of human-derived organic compounds in the environment represents a concrete risk of long-term environmental disaster.[1,2] Among the variety of organic pollutants, the occurrence of pharmaceuticals in aquatic and terrestrial environment increased

Abbreviations: API, active pharmaceutical ingredient; CYP, cytochrome P450; CYP116B5-fl, cytochrome 116B5 full length; CYP116B5-hd, cytochrome 116B5 heme domain; CYP116B5-SOX, fusion enzyme comprising cytochrome 116B5 heme domain and sarcosine oxidase; DSC, differential scanning calorimetry; KPi, inorganic potassium phosphate buffer; pNP, para-nitrophenol; pNC, para-nitrocatechol; SOX, sarcosine oxidase.

 © 2024 Wiley-VCH GmbH.

over the last few decades.[3] Hundreds of different human drugs have been reported as environmental contaminants, including antineoplastic agents, analgesics, and cardiac medications, and were detected in water bodies on global scale.[4,5] This outcome has been correlated to the incidental release of medications into effluent water from hospital and drug manufactures as well as farming and residential areas.[6,7] Approximately 30% of drugs were predicted to be potentially bioactive in aquatic organisms thus dangerous for wildlife,[8] particularly those which can interact with target receptor conserved among different species, such as antineoplastics agents.[9] Antineoplastics are not removed by the currently employed wastewater treatments and some of them, such as tamoxifen, have been detected over the toxicity value in surface-water in several countries.[9–12] Tamoxifen toxic effect on the endocrine system of aquatic organism and mammalians has been elucidated,[9,13–15] drawing attention to the hazardous nature of this drug as environmental pollutant and ecotoxic compound. The exploitation of bacterial cytochromes P450 (CYPs) for drugs conversion and drug metabolites production has been extensively investigated and produced excellent results.[16–20] *Acinetobacter radioresistens*' P450 116B5 showed to efficiently oxidize aromatic rings of APIs molecules such as tamoxifen and diclofenac. CYP116B5 is a Class VII cytochrome P450, indeed it is a catalytically self-sufficient single-polypeptide enzyme comprising a heme containing domain, as well as a reductase domain containing FMN and a 2Fe-2S cluster that require NADPH as a source of electrons (Figure 1). Although this enzyme maintains the typical characteristics of a monooxygenase, it can work as a peroxygenase.[21–31] In CYP116B5 catalytic route, the formation of the heme ferric hydroperoxy complex and the consequent oxoferryl π-cation radical (Compound I) is achievable by the direct binding of hydrogen peroxide to the heme ferrous iron.[21] The use hydrogen peroxide to drive the hemoproteins catalysis has been extensively studied,[29,32–38] and represents the most practical way to sustainably exploit them as biocatalysts. Indeed, by the addition of H_2O_2 as source of oxygen and electrons for the P450 catalytic cycle it is possible to avoid the use of the expensive cofactor(s) NAD(P)H and redox partner(s) reactions, that are often a source of uncoupling.[39] CYP116B5 heme domain (CYP116B5-hd) has been isolated by protein engineering and characterized for its ability to convert drugs using H_2O_2 as catalysis driving agent.[21] Nevertheless, the oxidative stress resulting from the use of H_2O_2 is disadvantageous for protein stability and toxic for cells.[40] In order to maximize the peroxygenase performance of the CYP116B5-hd, bypassing the limitations of the direct addition of hydrogen peroxide, we developed an in-situ H_2O_2 generating system to drive the CYP116B5-hd catalysis. For this purpose, the *Molecular Lego*[41–44] approach was exploited to design an artificially self-sufficient biocatalyst by fusing two enzymes of different species of origin, that is, the CYP116B5-hd from *Acinetobacter radioresistens* and the *Bacillus* sp. *B-0618* Sarcosine Oxidase (SOX)[45–50] which works as the H_2O_2 donor system, resulting in a fusion-enzyme chimera, able to self-generate H_2O_2 (CYP116B5-SOX) (Figure 1).[23] SOX from *Bacillus* sp. *B-0618* is a bacterial oxidoreductase that contains a covalently bound flavin that has already been proven to be successful as H_2O_2 donor partner for CYP152B1.[43] The main reaction catalyzed by SOX is the oxidative demethylation of the N-substituted amino acid sarcosine to yield glycine, formaldehyde, and hydrogen peroxide as by-product. Therefore, by using sarcosine as sacrificial substrate, we aim to use SOX as in-situ H_2O_2-generating system to carry out the peroxide driven catalysis of CYP116B5-hd, focusing on the regulation of P450 116B5 catalysis for drug bioconversion. Herein, we characterized the CYP116B5-SOX fusion enzyme[23] in terms of spectroscopical features, chemical, and thermal stability. We optimized the system catalysis using the P450 116B5 marker substrate *p*-nitrophenol, evaluating the kinetic parameters of the fusion enzyme. Finally, in order to investigate the potentiality of the engineered biocatalyst for bioremediation, we exploited a CYP116B5-SOX expressing *E. coli* strain to investigate the conversion of tamoxifen, a CYP116B5 substrate drug taken as a model of wastewater pollutant.

2 | MATERIALS AND METHODS

2.1 | CYP116B5-SOX gene design and expression vector construction

The coding sequence of the heme domain of CYP116B5 from *Acinetobacter radioresistens*[25] and that of SOX from *Bacillus* sp. *B-0618*[49] were used to build the gene coding for the CYP116B5-SOX fusion enzyme. The design approach followed for the construction of the fusion enzyme gene and the plasmid vector is similar to that previously reported by our laboratory.[43] In brief, the last triplet at 3' of the CYP116B5-hd gene has been fused to the first triplet at 5' of the SOX sequence through a 33 bp (Sequence 1) coding for a poly-glycine linker.

GGTCCAGGTGGCGGCGGTGGTGGCGGCCCAGGT (1)

AvrII and AscI restriction sites were inserted respectively at 5′ and 3′ of the linker sequence (Figure S1). A C-terminal 6xHis-Tag, useful for protein purification, were obtained by adding six CAC triplets in-frame between SOX last codon 3′ and TAA stop codon. The designed gene results in 2573 bp. The open reading frame of the gene is defined by an ATG triplet preceding the first codon of the CYP116B5 sequence. The CYP116B5-SOX gene were subcloned in a pET28a(+) vector between NcoI and EcoRI restriction sites (Figure S1), the gene insertion and plasmid construction were performed by GenScript (Piscataway, New Jersey).

2.2 | Protein expression and purification

CYP116B5-SOX was expressed as previously reported.[23] Cells were harvested and lysed by sonication (5 × 30 s pulses with a Misonix Ultrasonic Sonicator, Teltow, Germany) in 50 mM KPi at pH 6.8, 100 mM KCl, 1% Triton X-100 supplemented with 1 mg mL^{-1} lysozyme, 0.1 mg mL^{-1} DNAse I, and 1 mM PMSF. After 45 min ultracentrifugation at 40,000 rpm, the soluble fraction of cell lysate was loaded onto a 5 mL nickel-ion affinity column (His-trap HP, GE Healthcare) held at 25°C pre-equilibrated with the cell resuspension buffer and washed with 50 mM KPi at pH 6.8, 50 mM glycine after cell extract loading. The bounded

18607314, 2024, 5, Downloaded from https://analyticalsciencejournals.onlinelibrary.wiley.com/doi/10.1002/biot.202300664 by Universita Di Torino, Wiley Online Library on [14/05/2024]. See the Terms and Conditions (https://onlinelibrary.wiley.com/terms-and-conditions) on Wiley Online Library for rules of use; OA articles are governed by the applicable Creative Commons License

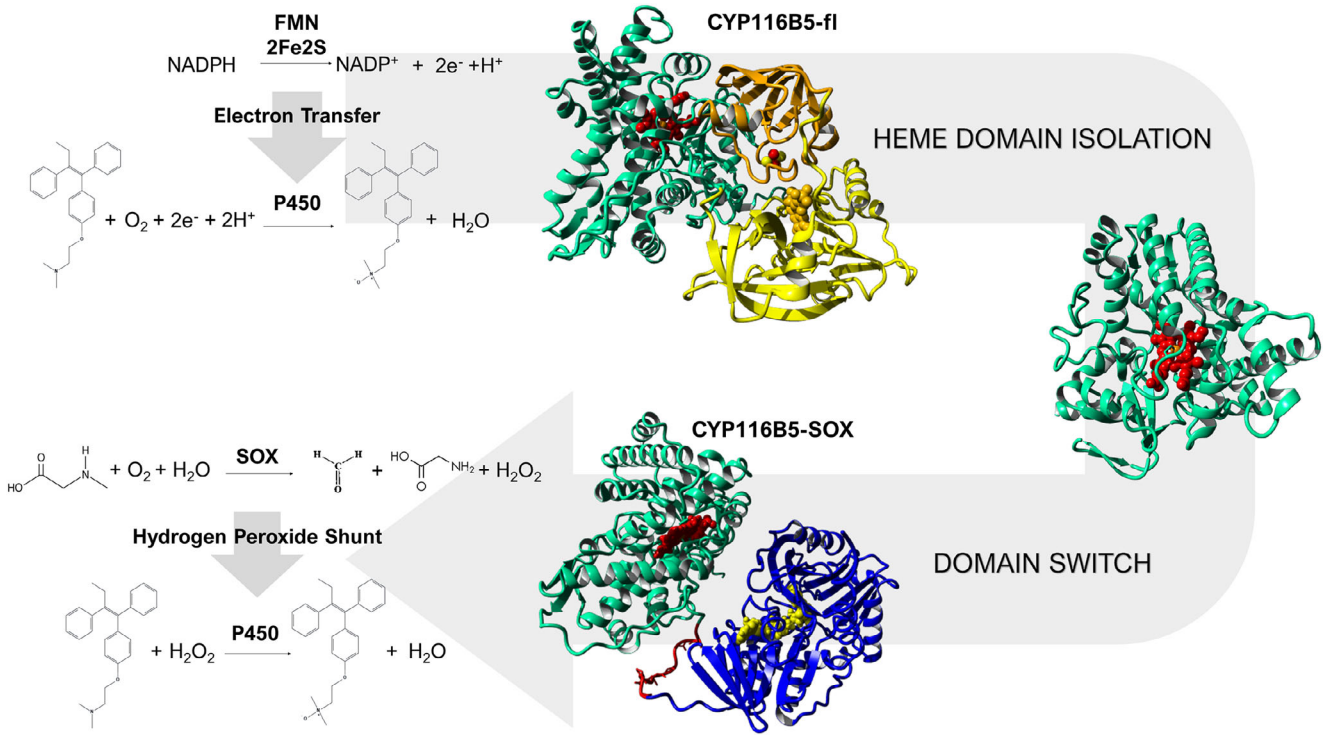

FIGURE 1 Outline of the process of protein engineering leading to design the CYP116B5-SOX fusion enzyme and reaction schemes of CYP116B5-fl and CYP116B5-SOX. The CYP116B5-fl (full length) catalyzes the NADPH-dependent conversion of drugs employing the reductase domain(s) consisting in a FMN binding domain and a 2Fe2S cluster. The CYP116B5-hd (heme domain) has been isolated and joined by domain switching to SOX (sarcosine oxidase). In the CYP116B5-SOX system the electron transfer mechanism is bypassed, as the P450 is driven by the peroxide-shunt mechanism, which only employs H_2O_2 as P450 cosubstrate. SOX is a bacterial oxidoreductase that contain a covalently bound FAD cofactor. The SOX's FAD is involved in the sarcosine oxidation to glycine and formaldehyde and the subsequent reduction of O_2 to H_2O_2, by which the FAD is regenerated in the oxidized form. Proteins secondary structure is represented as a ribbon model. CYP116B5 heme catalytic domain is colored in green, the FMN and the 2Fe2S center binding domains are colored in yellow and orange respectively, SOX is colored in blue. The CYP116B5-SOX linker is colored in red. Enzymes cofactors atoms are represented as balls. Protoporphyrin, FMN and FAD are colored in red, orange and yellow respectively. Iron atoms are represented as balls and colored in red. Sulfur atoms, when showed, are represented as balls and colored in yellow.

proteins were eluted applying a gradient 0–100 mM imidazole and collected in 1 mL fractions. The presence of P450-SOX was confirmed spectroscopically measuring the absorbance at 419 nm. Fractions containing the chimera were then further purified by size-exclusion chromatography (HiLoad 16/600 Superdex 200 pg) equilibrated with KPi buffer 50 mM pH 6.8 supplemented with KCl 200 mM.

2.3 | Fluorescence spectroscopy

The effect of sarcosine on CYP116B5-SOX fluorescence was analyzed using a Perkin-Elmer LS-5 spectrofluorimeter equipped with a thermostated cell holder. 3 μM of CYP116B5-SOX was dissolved in KPi 50 mM pH 6.8. The protein excitation spectra were recorded between 300 and 500 nm centering the analysis at the emission wavelength of 530 nm, whereas the emission spectra were recorded between 475 and 600 nm using the excitation wavelength at 450 nm. The protein fluorescence spectra were recorded for the oxidized protein, then sarcosine was added to a final concentration of 10 mM and spectra were recorded again for 2 h after sarcosine addition.

2.4 | Differential scanning calorimetry (DSC)

The thermal stability of CYP116B5-SOX and CYP116B5 full-length was evaluated by DSC. Experiments were carried out using a Microcal VP-DSC instrument (Malvern, UK) with a temperature gradient from 20°C to 75°C, at a scan rate of 75°C/h and 10 min of pre-scan equilibration.[51–53] The stability of proteins was investigated in potassium phosphate buffer at pH value of 6.8. All samples were run using 0.6 mg mL^{-1} enzyme. Data were analyzed using Microcal Origin software (Malvern, UK).

2.5 | Spectroscopic estimation of P450 domain hydrogen peroxide tolerance

P450 tolerance to H_2O_2 was investigated using Agilent 8453 UV–vis spectrophotometer and monitoring the CYP116B5-SOX UV-vis spectra maximum at λ at 419 nm over time at 15°C (Peltier Agilent 89,090 A). 3 μM of CYP116B5-SOX was suspended in KPi 50 mM at pH 6.8. The spectra of the enzyme were recorded before and after the addition

18607314, 2024, 5, Downloaded from https://analyticalsciencejournals.onlinelibrary.wiley.com/doi/10.1002/biot.202300664 by Universita Di Torino, Wiley Online Library on [14/05/2024]. See the Terms and Conditions (https://onlinelibrary.wiley.com/terms-and-conditions) on Wiley Online Library for rules of use; OA articles are governed by the applicable Creative Commons License

of either 1, 2, 3, 4, or 5 mM of H_2O_2 or 10, 50, 100, or 200 mM sarcosine over 30 min of incubation. The absorbance at 419 nm was plotted against time and data were fitted using a single exponential decay function (Equation 2) to obtain the decay rate constant (k) of the A_{419} in presence of H_2O_2.

$$y = y0 + a * e^{-k*x} \quad (2)$$

y: absorbance at 419 nm; x: time (min); k: decay rate constant (min^{-1}); a: original amount

2.6 | SOX domain residual activity after incubation with H_2O_2: formaldehyde quantification

In order to test the resistance of CYP116B5-SOX to H_2O_2 the residual activity of the two domains of the chimera was tested after incubation with H_2O_2. The SOX resistance was evaluated measuring the residual formaldehyde production after treatment with H_2O_2. 0.3 μM CYP116B5-SOX was incubated in KPi buffer at pH 6.8 in presence of 1, 3, 4, or 5 mM H_2O_2 or without H_2O_2 for 30 min at 25°C. After that, 250 mM of sarcosine was added to the solution and samples were incubated for 30 min at 30°C. The formaldehyde production was measured using a Formaldehyde Assay Kit (Sigma-Aldrich, St. Louis, MO 63103 USA). The reaction was stopped by the addition of 5% v/v trichloroacetic acid and 25% v/v Neutralizer solution was added to adjust the pH. After samples centrifugation for 10 min at 12,000 × *g*, 50 uL of each the reaction sample were mixed to 33 uL Reagent A and 22 uL Reagent B in a Nunc 96 wells plate and incubated at 25°C under total darkness to develop color. Blank was prepared mixing 33 μL Reagent A and 72 μL Kpi buffer. The formaldehyde was quantified basing on the absorbance at 370 nm as previously described.[54]

2.7 | CYP116B5 domain residual activity after incubation with H_2O_2: *p*-nitrocatechol production

CYP116B5-SOX was incubated at a concentration of 0.3 μM in KPi buffer at pH 6.8 in presence of 1, 2, 3, 4, or 5 mM H_2O_2 or without H_2O_2 for 30 min at 25°C. After that, 250 mM of sarcosine and 1 mM *p*-nitrophenol were added to the solution and samples were incubated for 30 min at 30°C. Reaction was stopped with 1% of trichloroacetic acid and *p*-nitrocatechol formation measured as described below.

2.8 | Optimization of the catalytic activity

The trials for CYP116B5-SOX activity were performed using L-sarcosine as SOX domain sacrificial substrate or, alternatively, H_2O_2 was directly added to CYP116B5-SOX to drive the P450 catalysis. *p*-nitrophenol (pNP) was used as marker substrate to test the CYP116B5 heme domain activity in the fusion enzyme. All reactions were carried out in 50 mM KPi buffer at desired pH. For the identification of the optimal concentration of sarcosine 0.25 μM enzyme were mixed with 1 mM pNP and 1, 10, 100, 250, 300, or 500 mM sarcosine and incubated for 30 min at a pH value of 6.8. For the investigation of the activity at different pH, potassium phosphate buffer was used to reach desired pH during catalysis. Concentrations of two potassium phosphate salts (K_2HPO_4 and KH_2PO_4) were modulated to obtain pH value of 5, 5.6, 6.2, 6.8, 7.4, 8, 8.5, 8.7 respectively, reaction were performed using 0.25 μM enzyme 1 mM pNP, and either 250 mM sarcosine or 1 mM H_2O_2 and incubated over 30 min. The kinetic parameters for the production of p-nitrocatechol (pNC) were obtained by mixing 0.25 μM CYP116B5-SOX, 250 mM sarcosine with pNP at a concentration of 0, 0.05, 0.1 0.2, 0.6, 1.2, 1.6, or 2.0 mM respectively, reactions were performed at a pH value of 7.4 and stopped after 5 min. All reactions were started by sarcosine or H_2O_2 addition and were kept at 30°C for the due time. After addition of 1% vol/vol of trichloroacetic acid to terminate the reaction, each sample was centrifuged at 12,500 × *g* for 10 min to remove unsoluble denatured enzyme. The *p*-nitrocatechol produced by the CYP116B5 domain[21] was evaluated spectroscopically measuring the absorbance at 515 nm ($\varepsilon = 12.4\ mM^{-1}\ cm^{-1}$) right after sample color development, obtained by addition of NaOH 0.9 M to adjust the pH.

2.9 | Hydrogen peroxide quantification

In order to quantify the H_2O_2 accumulated in solution during the CYP116B5-SOX reaction, a horseradish peroxidase (HPR) coupled reaction was used. [43] A calibration curve was obtained by mixing 50 mM KPi at pH 7.4, 0.5 μM HPR, 250 μM ABTS, and either 10, 25, 50, 75, or 0 μM H_2O_2 in a quartz cuvette and measuring the end-point absorbance at 650 nm associated to the production of $ABTS^{\bullet+}$.[55] The same HRP and ABTS concentration and buffer conditions were used to quantify the H_2O_2 in the CYP116B5-SOX reaction samples. In order to investigate the H_2O_2 production overtime HRP, ABTS, and KPi were mixed with 5 mM sarcosine, reaction was started by the addition of 5 nM CYP116B5-SOX and incubated for 20 min. Measurements were taken every 5 s using an Agilent 8453 UV–vis spectrophotometer (diode array) at the controlled temperature of 30°C (Peltier Agilent 89,090 A). A reaction was prepared using the same condition with the addition of 20 μM *p*-nitrophenol and analyzed following an identical procedure. All measurements were made in triplicate.

2.10 | Drugs bioconversion in whole cells

Drugs bioconversion was performed using a *E. coli* BL21 (DE3) strain transformed with the pET-28-a-CYP116B5-SOX(+) expression vector. The cell growth and protein expression were performed as reported in the Materials and Methods section. Cells were harvested 24 h after protein expression induction by centrifugation at 4000 × *g* for 30 min. Cells, at a final optical density of 10 at 600 nm, were resuspended in KPi buffer 0.1 M at a pH value of 7.5 supplemented with 1 mM tamoxifen.

18607314, 2024, 5, Downloaded from https://analyticalsciencejournals.onlinelibrary.wiley.com/doi/10.1002/biot.202300664 by Universita Di Torino, Wiley Online Library on [14/05/2024]. See the Terms and Conditions (https://onlinelibrary.wiley.com/terms-and-conditions) on Wiley Online Library for rules of use; OA articles are governed by the applicable Creative Commons License

For the study of tamoxifen conversion yield, sarcosine was added to the cell suspension at a final concentration of either 5, 20, 20, 50, 100, 200, 250, 500, or 1000 mM. Alternatively, 0.5, 1, 5, or 10 mM hydrogen peroxide was used. After sample extraction with 50% v/v ethyl acetate, the organic phase was collected and Tamoxifen metabolites were analyzed using an HPLC coupled with a diode array UV detector (Agilent-1200, Agilent technologies, Santa Clara, CA, USA) set at 276 nm applying a 360 nm correction. A C18 prepacked column (Phenomenex-Kinetex Core Shell) was used, the chromatographic separation was performed in isocratic conditions using 82% methanol and 18% triethylamine (1% v/v) as mobile phase.

3 | RESULTS

3.1 | Design, expression, and purification of CYP116B5-SOX

In order to obtain a biocatalyst able to perform in-situ H_2O_2 generation we designed the gene of the fusion enzyme joining the coding sequence of CYP116B5-hd from *Acinetobacter radioresistens* with the Monomeric Sarcosine Oxidase gene from *Bacillus* sp. *B-0618* through a Gly-Pro-$(Gly)_7$-Pro-Gly linker (Figure 1, S1).[23] A poly glycine sequence was used in order to allow the highest possible flexibility of the loop connecting the two domains.[43] Indeed, the low steric hindrance of glycine residues within the linker was previously shown to support conformational rearrangements and allow correct folding of the fusion protein.[43] The heterologous expression of CYP116B5-SOX was performed in *E. coli* BL21 (DE3) transformed with the pET-28-a-CYP116B5-SOX(+) vector. The purification of the engineered C-terminal 6xHis-tagged protein was performed using immobilized metal affinity chromatography (IMAC), followed by size exclusion chromatography (SEC). The resulting purified CYP116B5-SOX protein showed a single band around 95,000 Da on SDS-PAGE, consistent with the predicted molecular mass of 95,913 Da (His-Tag included) (Figure 2A). Moreover, when exposed to UV light, the 95,000 Da SDS-PAGE band was found to emit light in the visible wavelength range (Figure 2A). This distinctive behavior indicates the presence of a fluorophore bound to the protein even in the electrophoresis denaturing condition.[56] Indeed, SOX FAD cofactor is known to be covalently bound to the poly-peptide chain of the protein through the sulfur atom of a cysteine residue near the COOH-terminus of the protein (8α-S-cysteinyl-FAD).[45,46,57] The fluorescence of the polyacrylamide gel band is thereby in line with a proper SOX domain maturation process within the fusion enzyme. The protein purity was evaluated spectrophotometrically, the batch of the purest fusion enzyme was found to display a A_{419}/A_{280} of 0.53. The yield of protein after purification was 10.62 mg L^{-1} of cell colture, based on the 450 nm absorbance after CO binding, that is 5 times that obtained by our laboratory for the CYP116B5-fl (2.06 mg L^{-1} of cell culture) and comparable to that of CYP116B5-hd (11.22 mg L^{-1}). The data indicate that the presence of the partner domain SOX in the artificial fusion enzyme does not negatively affect the amount of the folded protein, as instead it was observed for the CYP116B5-fl.

3.2 | Spectroscopical characterization

The single domains within the fusion proteins were both characterized in terms of cofactor incorporation and reactivity using absorbance and fluorescence spectroscopy. The UV-vis absorption spectrum of CYP116B5-SOX in steady state displays the typical spectroscopic features of CYP116B5 heme domain oxidized form,[21] that is, the Soret peak at 419 nm and two absorbance Q-bands at 539 and 573 nm, with another maximum around 356 nm, as expected for the six-coordinate low-spin state ferrous-heme form (Figure 2B).[21] Within the fusion protein spectrum we observed the characteristic flavoprotein absorption bands with maxima at 454 (ε_{454nm}: 12,200 M^{-1} cm^{-1}) and a shoulder at 475 nm (Figure 2B).[46] After reduction with sodium dithionite the protein showed a decrease of the Soret peak intensity and a shift to 410–411 nm as well as the merging of the Q-bands into a single band at 550 nm, in line with the heme $Fe^{III} \rightarrow Fe^{II}$ transition,[58] concomitantly it was observed the decrease of the 454 nm and 475 nm bands, due to the SOX reduction.[48] The protein sample in the reduced state was bubbled with carbon monoxide, resulting in the typical Soret peak conversion to 450 nm (ε_{450nm}: 91,000 M^{-1} cm^{-1}),[21] as expected for the Fe^{II}-CO complex formation (Figure 2B).[59] Due to the lower molar extinction coefficient (ε) of SOX compared to the CYP116B5-hd and the overlapping absorbance of FAD and heme in the visible region, an adequate spectral characterization of SOX wasn't achievable using only UV-VIS spectroscopy. Therefore, fluorescence was used to characterize the spectral properties of the fusion enzyme SOX domain. Figure 2C shows the fluorescence excitation and emission spectra of the fusion protein SOX domain. In fully aerated conditions the excitation spectra of the enzyme showed maxima at 372 nm, 454 nm, and a shoulder at 475 nm, measuring the light emitted by the sample at 530 nm. Right after addition of a strong excess of sarcosine ($>10^3$ molar equivalents) the fluorescence intensity at λ_{530} decreased, indicating the reduction of the SOX FAD (Figure 2C). SOX covalent 8α-S-cysteinyl-FAD is known to undergo specific spectral changes similar to those of free FAD when reduced by a two-electron transfer process.[48] In our experimental conditions, the complete bleaching of the SOX fluorescence could not be observed, likely due to the oxidizing environment that leads to immediate oxygen incorporation by the cofactor after reduction. The complete re-oxidation of SOX was reached 2 h after the addition of sarcosine (Figure 2C) and this is fully in line with the catalytic cycle of SOX.[48] Indeed, the concentration of oxygen in solution in air-saturated buffer condition (approximately 0.27 mM) is known to be rate-limiting for SOX catalysis[48] whereas the reductive semi-reaction proceeds at much higher rate (rate of reductive half-reaction = 140 s^{-1} at pH 8.0, 25°C).[50] Overall, the spectroscopic characterization of the fusion enzyme confirmed the correct cofactors incorporation and reactivity after the expression and purification of the enzyme. The data indicate that both CYP116B5

18607314, 2024, 5, Downloaded from https://analyticalsciencejournals.onlinelibrary.wiley.com/doi/10.1002/biot.202300664 by Universita Di Torino, Wiley Online Library on [14/05/2024]. See the Terms and Conditions (https://onlinelibrary.wiley.com/terms-and-conditions) on Wiley Online Library for rules of use; OA articles are governed by the applicable Creative Commons License

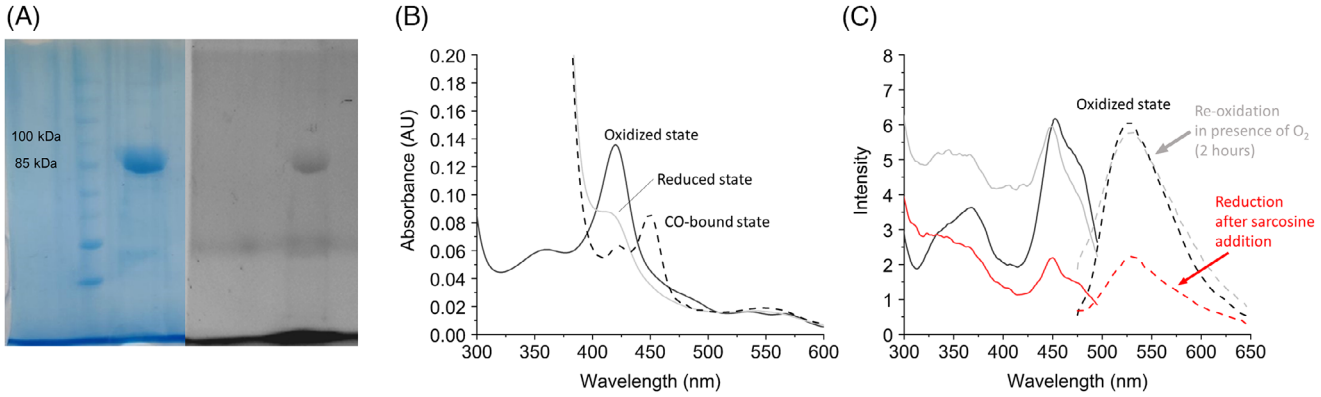

FIGURE 2 (A) SDS-PAGE of CYP116B5-SOX purified by IMAC followed by size-exclusion chromatography. The polyacrylamide was colored using a Comassie blue protein stain (Giotto Biotech S.r.l, Firenze, Italy) (left) or exposed to UV-light by transillumination to detect protein bands fluorescence (right). MW ladder: 200, 150, 120, 100, 85, 70, 60, 50, 40 kDa. (B) Spectra of 1.5 μM CYP116B5-SOX in KPi 50 mM at pH 6.8 displaying the spectral properties of the heme oxidized form (black solid line), reduced form in presence of sodium dithionite (gray solid line), and CO-bound form after carbon monoxide bubbling (black dashed line). (C) Fluorescence excitation (solid lines) and emission (dashed lines) spectra of 3 μM CYP116B5-SOX in fully aerated condition in presence of sarcosine. Data shows the spectral properties of flavin oxidized form (black lines), two-electron reduced form right after the addition of 10 mM sarcosine (red lines), and re-oxidized form 2 h after sarcosine addition (gray lines).

and SOX functionalities are conserved in the artificial CYP116B5-SOX fusion enzyme.

3.3 | Thermal denaturation

The thermal stability of the enzyme was studied by using DSC. In CYP116B5, class VII P450 from *Acinetobacter radioresistens*, the heme domain is naturally fused to the reductase domain.[23,25] We investigated the thermal denaturation of full-length CYP116B5 (CYP116B5-fl) as a function of pH, from 5.8 to 8.0 (Figure S2, Table S1). The previously characterized CYP116B5-hd[21] allowed to readily identify the unfolding transition of the heme domain, which corresponded to the main peak in the thermogram (Figure S2), while the smaller peak at T > 50°C corresponded to the reductase domain. The heme domain unfolds with a T_M between 42.8 and 45.6°C as a function of the pH employed (Figure S2, Table S1). At pH 6.8 the best compromise between stability (measured by T_M = 45.0°C) and amount of folded protein (measured by enthalpy = 167,600 cal mol^{-1}) was found. Therefore, at pH 6.8 the enzyme finds the best conditions in terms of protein homogeneity and thermal stability. Previously, pH 6.8 was also selected as the best conditions for the isolated heme domain.[21] Thereby, since the full-length form of the enzymes also shows higher stability at this pH this value was used to investigate the thermal denaturation of CYP116B5-SOX. The artificial fusion enzyme displays a high energy barrier to denaturation, as shown by the T_M of the CYP116B5-hd which was 48.4 ± 0.04°C with an enthalpy value of 175,500 ± 1850 cal mol^{-1}, and 58.3 ± 0.02°C and 120,500 ± 1350 cal mol^{-1} for the SOX domain respectively (Figure 3). The P450 domain displayed a 3.4°C increased T_M in the artificial fusion enzyme compared to the CYP116B5-fl, and similar to the T_M of the heme isolated form (T_M of CYP116B5-hd = 48.2°C).[21] Furthermore, the enthalpy associated to the heme domain denaturation in the CYP116B5-SOX system was higher compared to the CYP116B5-fl, indicating a larger amount of folded enzyme and a good homogeneity of the protein. The SOX domain showed a lower T_M in the CYP116B5-SOX compared to the previously reported data. Indeed, the reported T_M of native SOX is 64.0°C.[60,61] and the SOX domain displayed a T_M of 63.2 ± 0.02°C when used in other fusion enzymes recently reported by our laboratory.[43] Overall data indicate that the native folding state of CYP116B5 heme domain and the SOX domain was conserved in the CYP116B5-SOX fusion enzyme.

3.4 | CYP116B5-SOX stability using different H_2O_2 supply systems

The objective of this work is to achieve continuous supply of H_2O_2 generated by SOX to drive the P450 catalysis, therefore it is crucial to define the stability of the CYP116B5-SOX heme domain toward H_2O_2. Indeed, the oxidative damage caused by hydrogen peroxide in solution is known to affect the structure and reactivity of enzymes. In the case of P450s, H_2O_2 causes oxidative damage to the protein structure as well as to protoporphyrin, leading to the oxidation of the heme-thiolate cysteine to sulfenic acid and loss of catalytic performance. The decrease of heme absorbance is thus associated to the cofactor loss and the enzyme inactivation.[21,40,62,63] The CYP116B5-SOX heme domain H_2O_2 tolerance was assessed by monitoring the decreasing of the Soret band absorbance at 419 nm over time, that is associated to protein oxidative damage in presence of H_2O_2 either directly added in solution or produced starting from sarcosine employing the SOX supply system. The data are reported in Table 1 and Figure 4. The CYP116B5-SOX heme domain tolerance to H_2O_2, in terms of A_{419} decay rate and total amplitude of decrease, was found to be in

18607314, 2024, 5, Downloaded from https://analyticalsciencejournals.onlinelibrary.wiley.com/doi/10.1002/biot.202300664 by Universita Di Torino, Wiley Online Library on [14/05/2024]. See the Terms and Conditions (https://onlinelibrary.wiley.com/terms-and-conditions) on Wiley Online Library for rules of use; OA articles are governed by the applicable Creative Commons License

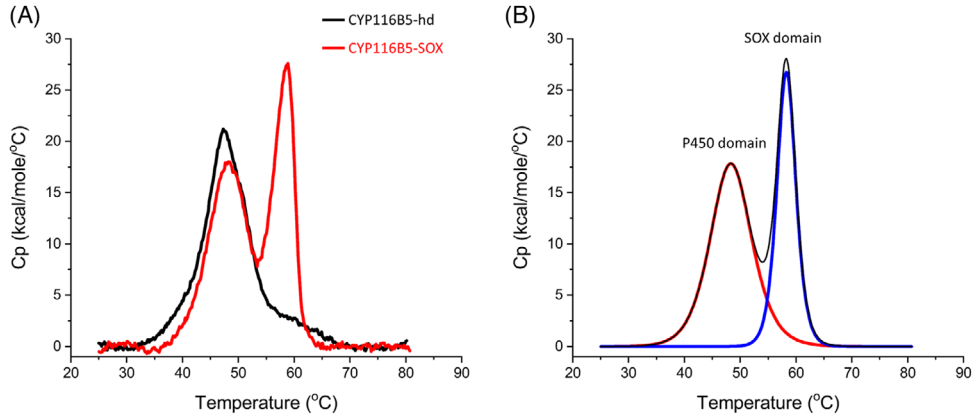

FIGURE 3 Differential scanning calorimetry of CYP116B5-SOX, analysis was carried out at scan/rate of 75°C/h, at pH value of 6.8 in 50 mM KPi buffer. (A) experimental curves of CYP116B5-SOX (red line) and CYP116B5-hd (black line) thermal denaturation. (B) fitting of the CYP116B5-SOX experimental curve applying a non-two-state denaturation model (black line) and deconvolution of the first peak (red line) and of the second peak (blue line).

TABLE 1 Hydrogen peroxide tolerance of CYP116B5-SOX using different H^2O^2 supply methods.

	CYP116B5-SOX		CYP116B5-hd[21]			CYP116B5-SOX	
H_2O_2	k (s^{-1})	A (%)	k (s^{-1})	A (%)	Sarcosine	k (s^{-1})	A (%)
1 mM	0.0009	2.3 ± 0.4	n/a	4.2 ± 0.9	**10 mM**	n/a	3.6 ± 2.1
2 mM	0.0010	6.8 ± 2.1	0.0024	7.2 ± 1.9	**50 mM**	n/a	2.8 ± 1.1
3 mM	0.0019	7.3 ± 1.1	0.0034	7.1 ± 2.9	**100 mM**	n/a	4.3 ± 0.7
4 mM	0.0022	9.5 ± 0.6	0.0042	5.1 ± 1.9	**200 mM**	n/a	4.4 ± 0.8
5 mM	0.0035	11.0 ± 2.6	0.0051	10.2 ± 0.8			

Note: Decay rate constant (k) and amplitude of decrease (A) of the P450 absorbance band at λ419 were analyzed incubating 3 μM of enzyme at 15°C, pH 6.8 over 30 min in presence of increasing concentration of H_2O_2 or sarcosine. Data are compared to the previously reported CYP116B5-hd stability toward H_2O_2.[21]

general similar or higher when compared to the isolated heme domain (Table 1).[21] When a solution containing CYP116B5-SOX enzyme is mixed with sarcosine in presence of O_2, H_2O_2 is continuously produced by SOX catalysis (Supplementary, Figure 4S).[43,48] In this case the absorbance decreasing over the course of time could not be fitted to the same exponential decay equation used in the previous case, likely because of the attenuated damage granted by a continuous increment rather than a instantaneous addition of H_2O_2, consequently this also beneficially impacts the overall amplitude of heme inactivation (Table 1, Figure 4). In any case, using a concentration of sarcosine up to 200 mM, the total protein loss did not exceed the 4.4 ± 0.8% (Table 1). The unusual stability of CYP116B5-hd to the oxidative damage induced by H_2O_2 has already been reported.[21] Our observation further confirmed the CYP116B5-hd stability in presence of hydrogen peroxide in solution in the context of the fusion enzyme. Moreover, our data suggest that when the enzyme is mixed with sarcosine even in large concentration excess, implying H_2O_2 production at its maximum potential,[48] the overall protein loss is almost negligible. The data indicate an excellent chemical stability of the fusion enzyme when the SOX is employed as H_2O_2-donor.

3.5 | Effect of H_2O_2 on the CYP116B5-SOX single domains activity

The protein stability during the reaction is a crucial issue for the feasibility of a self-sufficient system based on H_2O_2 generation. In particular, the effect of H_2O_2 on the enzyme catalytic performance was evaluated for both the SOX and CYP116B5 domains of the fusion enzyme. The stability of the enzyme to the peroxide was evaluated in terms of residual activity of the CYP116B5-SOX after incubation with H_2O_2. This was calculated for both the domains using the full activity of the enzyme not treated with H_2O_2 as term of comparison. The activity of the SOX domain was estimated on the basis of the accumulation of formaldehyde, that is one of the byproducts of the SOX catalysis during sarcosine oxidation. As expected, the SOX domain didn't show any decrease in the catalytic performance when exposed to up to 5 mM of H_2O_2 over 30 min (Figure 4E). In our experiments, the amount of H_2O_2 produced by CYP116B5-SOX at its full rate over 20 min was 3.70 ± 0.14 mM (Figure S4). According to our data, the above mentioned concentration of peroxide accumulated during the reaction of CYP116B5-SOX shouldn't significantly affect

18607314, 2024, 5, Downloaded from https://analyticalsciencejournals.onlinelibrary.wiley.com/doi/10.1002/biot.202300664 by Universita Di Torino, Wiley Online Library on [14/05/2024]. See the Terms and Conditions (https://onlinelibrary.wiley.com/terms-and-conditions) on Wiley Online Library for rules of use; OA articles are governed by the applicable Creative Commons License

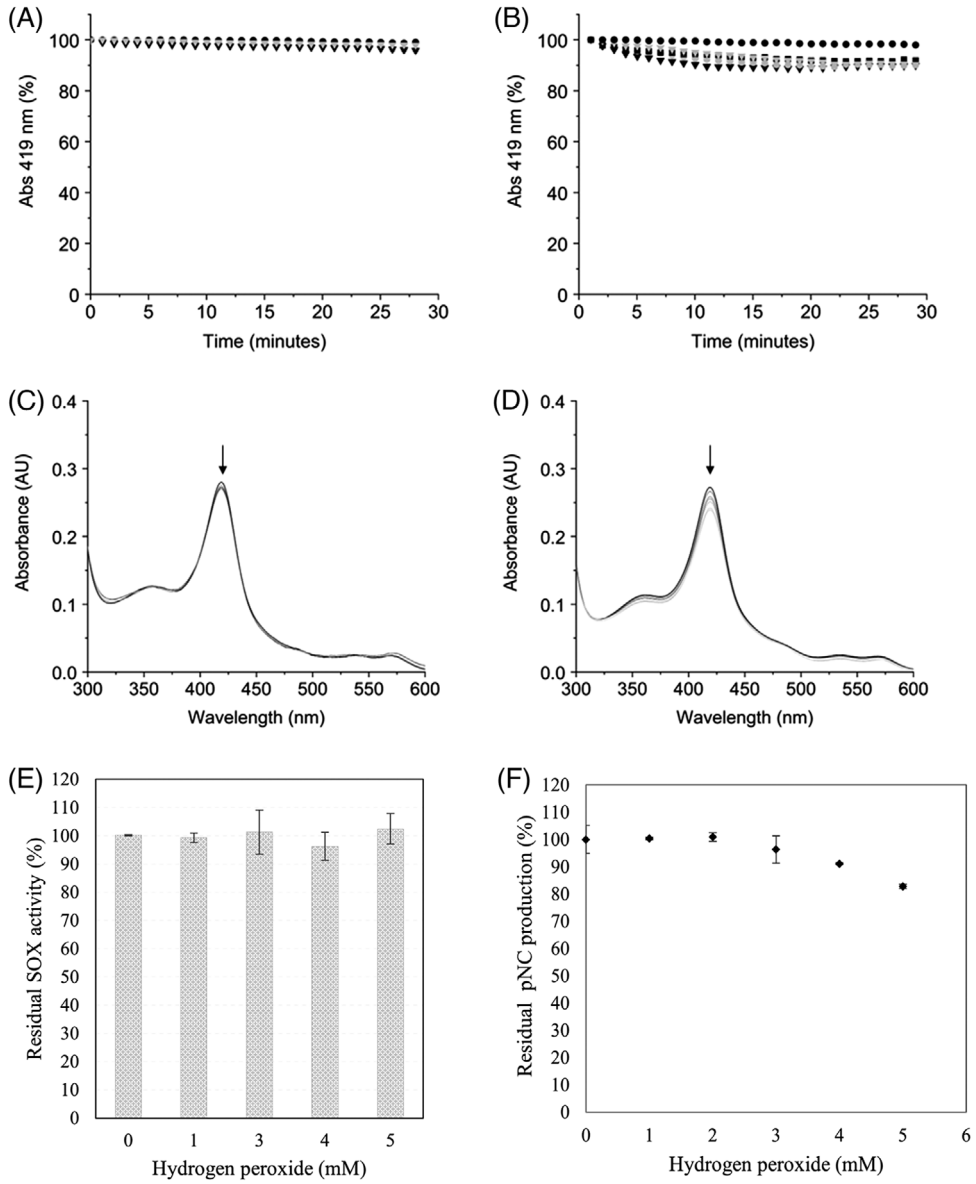

FIGURE 4 Hydrogen peroxide tolerance of CYP116B5-SOX. (A, B, C, D) P450 absorbance decrease due to oxidation of the heme-thiolate ligand mediated by H_2O_2, either produced by SOX (A, C) or added in solution (B, D). (A, B) λ419 nm absorbance decay percentage over 30 min of CYP116B5-SOX in KPi at pH 6.8 in presence of (A) sarcosine at a concentration of 10 mM (gray triangles), 50 mM (black circles), 100 mM (black triangles), and 200 mM (gray circles) or (B) H_2O_2 at a concentration of 1 mM (black circles), 2 mM (gray triangles), 3 mM (black squares) 4 mM (gray circles), and 5 mM (black triangles). (C, D) CYP116B5-SOX UV–vis spectra recorded over 30 min at 15°C after the addition of (C) 200 mM sarcosine or (D) 5 mM H_2O_2. Protein concentration was 3 μM, arrows show the direction of the observed spectral change. (E, F) Residual activity of the two domain of the fusion enzyme after incubation with H_2O_2. Sample were incubated 30 min at 25°C in presence of different concentrations of H_2O_2. The activity of the enzyme treated with H_2O_2 was compared to a not treated sample, used to define the total activity of the enzyme. (E) Activity of SOX domain evaluated as the formaldehyde produced by CYP116B5-SOX after 30 min in presence of 250 mM sarcosine. (F) Activity of CYP116B5-SOX expressed as *p*-nitrocatechol production after 30 min in presence of 250 mM sarcosine and 1 mM *p*-nitrophenol. All reaction were performed in triplicate, error bands represent the standard deviation.

the SOX performance. The P450 domain activity was expressed as the amount of *p*-nitrocatechol produced by CYP116B5-SOX using sarcosine as co-substrate (Figure 4F). The enzyme meantained more than 96% of the total activity when treated with up to 3 mM H_2O_2, and about the 82% up to 5 mM. The data confirm the overall high resistance of the P450 116B5 to hydrogen peroxide.[21] Interestingly, at the higher concentration of H_2O_2 (5 mM) the P450 heme-thiolate ligand oxidation measured in our spectrophotometry experiments was only the 11% (Figure 4B, Table 1). This probably suggests that the loss of activity for the *p*-nitrocatechol production is due to both the heme coordination loss and the oxidative damage of H_2O_2 against the heme domain protein structure,[40] which would explain the slight difference between the cofactor loss and the observed overall decrease of catalytic performance of the fusion enzyme.

18607314, 2024, 5, Downloaded from https://analyticalsciencejournals.onlinelibrary.wiley.com/doi/10.1002/biot.202300664 by Universita Di Torino, Wiley Online Library on [14/05/2024]. See the Terms and Conditions (https://onlinelibrary.wiley.com/terms-and-conditions) on Wiley Online Library for rules of use; OA articles are governed by the applicable Creative Commons License

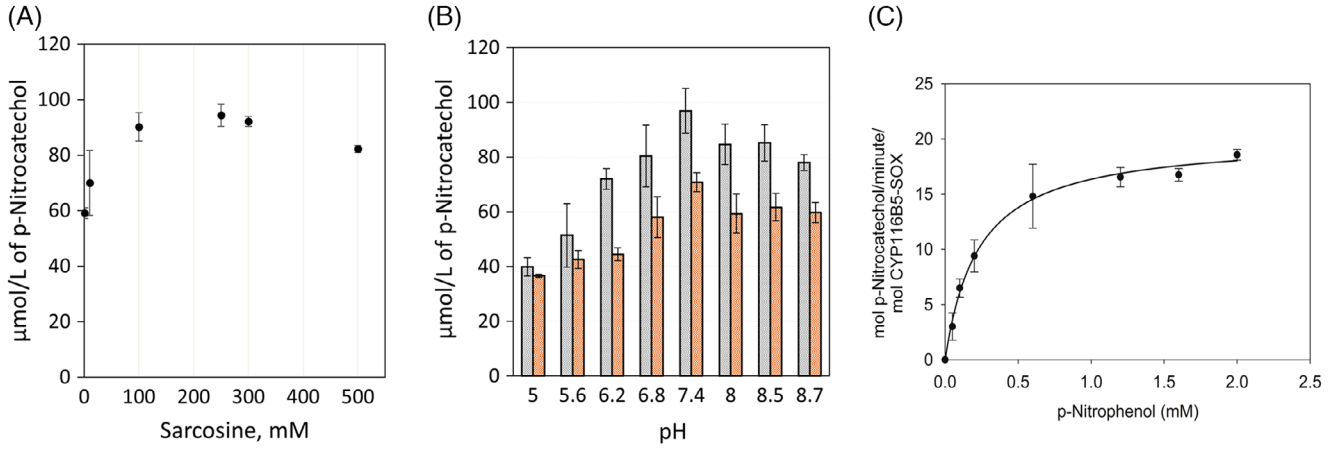

FIGURE 5 CYP116B5-SOX catalysis investigation for the production of p-nitrocatechol. (A) Investigation of the optimal concentration of sarcosine. 0.25 µM enzyme were mixed with 1 mM pNP and 1, 10, 100, 250, 300, or 500 mM sarcosine and incubated for 30 min at a pH value of 7.4. (B) Fusion enzyme activity at different pH. reaction were performed using 0.25 µM enzyme 1 mM pNP, and either 250 mM sarcosine (gray columns) or 1 mM H_2O_2 (orange columns) and incubated for 30 min at 30°C. (C) Michaelis-Menten fitting of the rate of production of pNC at increasing concentration of substrate. Reactions were performed using 0.25 µM CYP116B5-SOX, 250 mM sarcosine with pNP at a concentration of 0, 0.05, 0.1 0.2, 0.6, 1.2, 1.6, or 2.0 mM respectively, samples were incubated for 5 min at 30°C and a pH value of 7.4.

3.6 | Fusion enzyme catalysis

In order to optimize the experimental conditions for the CYP116B5-SOX catalysis, we investigated the catalytic performance of the purified enzyme for the conversion of the marker substrate *p*-nitrophenol (pNP). P450 116B5 is known to perform the peroxide-driven hydroxylation of pNP into *p*-nitrocatechol (pNC), that is easily detectable by the distinctive 515 nm absorbance band measurable in alkaline conditions.[21,58] The optimal sarcosine concentration needed to drive the CYP116B5-SOX catalysis was determined by measuring the production of pNC driven by sarcosine ranging from 1 to 500 mM (Figure 5A). The CYP116B5-SOX showed an increased rate for pNC production up to 250 mM sarcosine. A further increase in sarcosine concentration led to an apparent decrease of the rate of production of pNC. This effect can be ascribed to the accumulation of H_2O_2 produced by SOX, resulting in enzyme damage and subsequent loss of catalytic efficiency,[43] as suggested also by our investigation of the enzyme residual activity after H_2O_2 exposure (Figure 4F). For this reason all the subsequent experiments were carried out using either 250 mM sarcosine or keeping constant the sarcosine / CYP116B5-SOX molar ratio. The optimal pH condition for the CYP116B5-SOX catalysis was assessed by measuring the production of pNC as a function of pH value used, ranging from 5.0 to 8.7. In this case, two H_2O_2 supply method were employed, that is, the direct addition of H_2O_2 in solution or the in-situ generation of H_2O_2 by SOX domain driven by sarcosine (Figure 5B). Data show that, regardless the supply method used, the CYP116B5-SOX display the highest catalytic performance at pH value of 7.4. At this slightly alkaline pH CYP116B5-SOX produced 96.9 ± 8.2 or 70.9 ± 3.5 µmoles L^{-1} of pNC when the catalysis was driven by sarcosine or exogenous H_2O_2 respectively. Of note, for each pH condition tested, the sarcosine-driven CYP116B5-SOX catalysis resulted in a higher a production of pNC compared to the direct addition of exogenous a H_2O_2 (Figure 5B). This data is in line with a better regulation of the P450 catalysis obtained promoting a continuous production of hydrogen peroxide exploiting the SOX catalysis as supply system. The kinetic parameters for the CYP116B5-SOX activity toward pNP were extrapolated by fitting the rate of pNC production at increasing concentration of substrate to the classical Michaelis-Menten equation (Figure 5C). CYP116B5-SOX showed a k_{cat} of 20.1 ± 0.6 min^{-1} and a K_M of 0.23 ± 0.03 mM when the optimal reaction condition were applied, resulting in about 4x higher specificity constant (k_{cat}/K_M) compared to the isolated CYP116B5-hd (k_{cat} of 2.65 ± 0.14 min^{-1}; K_M of 0.129 ± 0.30 mM).[21] Overall, the data indicate the excellent catalytic behavior of the engineered H_2O_2 self-generating fusion enzyme system. Indeed, when the catalysis of the CYP 116B5-SOX was driven by sarcosine, thus the in-situ production of H_2O_2 was employed, the P450 showed an increased activity compared to both the exogenous peroxide-driven CYP116B5-SOX and the isolated CYP116B5-hd (Figure 5). This positive effect on the P450 activity could be driven by the modulation of the hydrogen peroxide accumulation in solution, which is controlled by the SOX domain and results in a higher stability and a better sustained catalysis of the heme domain in the fusion enzyme system.

3.7 | Hydrogen peroxide production during CYP116B5-SOX reaction

In our fusion enzyme system, the SOX domain is exploited for the continuous production of H_2O_2 to sustain the peroxygenase activity of the CYP116B5-SOX. We measured the amount of H_2O_2 accumulated in solution by SOX activity over time. Optimal enzyme, substrate and co-substrate (sarcosine) concentrations were selected on the basis of the conditions that yielded higher *p*-nitrocatechol production. We measured the accumulation of H_2O_2 in real time coupling

18607314, 2024, 5, Downloaded from https://analyticalsciencejournals.onlinelibrary.wiley.com/doi/10.1002/biot.202300664 by Universita Di Torino, Wiley Online Library on [14/05/2024]. See the Terms and Conditions (https://onlinelibrary.wiley.com/terms-and-conditions) on Wiley Online Library for rules of use; OA articles are governed by the applicable Creative Commons License

the CYP116B5-SOX reaction to the horseradish peroxidase activity, which uses H_2O_2 to convert ABTS into a colored product (ABTS•$^+$) (Figure S4).[43,55] The data indicate that the CYP116B5-SOX produced 1.308 mM ± 0.038 mM after 5 min of reaction, that is the time used in our experiment to extrapolate the kinetics parameter for the conversion of *p*-nitrophenol, and up to 3.650 ± 0.136 mM over 20 min. As expected, in the presence of *p*-nitrophenol, the peroxygenase activity of the CYP116B5 consumed only 3.2% of the H_2O_2 accumulated (Figure S4), that is fully in line with the concentration of *p*-nitrocatechol produced in the same condition (about 100 μM) and measured during our experiments (Figure 5). The data suggest that the H_2O_2-donor functionality is able to sustain the peroxygenase activity of the P450 and that the H_2O_2 consumption of the CYP116B5-SOX is entirely coupled with the formation of the product.

3.8 | Drugs bioconversion using CYP 116B5-SOX expressing *E. coli* strain

In order to study the applicability of the fusion enzyme catalysis in bioremediation we performed a reaction scale-up exploiting a strain of *E. coli* BL21 (DE3) cells transformed with the pET-28-a-CYP116B5-SOX(+) vector: *E. coli (CYP116B5-SOX)*. We employed the transformed bacteria as biocatalytic system to remove tamoxifen,[64–73] commonly reported as water pollutant,[9] from an aqueous buffered medium, taken as a model of contaminated water. We used HPLC-MS to identify the metabolites produced by CYP116B5-SOX catalysis. Purified CYP116B5-SOX (where catalysis is driven by sarcosine) and CYP116B5-*hd* (where catalysis is driven by H_2O_2) were both found to convert tamoxifen into the corresponding *N*-desmethyl metabolite—as already reported[21]— and the *N*-oxide metabolite (Figure S5). Nevertheless, the main metabolite detected after the extraction of the samples from the whole cell batch during the bioconversion process using *E. coli (CYP116B5-SOX)* as biocatalyst was tamoxifen *N*-oxide (Figure 6). Therefore we investigated the performance of the transformed cells strain for the tamoxifen bioconversion by measuring the end-point yield of production of tamoxifen *N*-oxide, after 24 h. incubation in presence of either increasing concentration of sarcosine or H_2O_2 as catalysis driving agent (Figure 7). The fusion enzyme system was able to convert tamoxifen using both the H_2O_2 supply method. When the *E. coli (CYP116B5-SOX)* cells activity was analyzed as a function of the sarcosine concentration in the reaction medium, the system showed the maximal performance when the reducing agent was kept at a concentration in a 100–250 mM range (Figure 7B). The higher yield of tamoxifen conversion was reached at a concentration of 250 mM of sarcosine, where the whole cell catalysis resulted in the production of 239 ± 20 μM tamoxifen *N*-oxide, corresponding to about the 25% conversion of initial tamoxifen amount, as compared to only the 2% with H_2O_2 direct addition (Figure 7). In general, when *E. coli (CYP116B5-SOX)* cells were supplemented with sarcosine, the performance of the biocatalyst was found to be better than adding directly hydrogen peroxide in solution. *E. coli (CYP116B5-SOX)* cells showed about a 12-folds higher performance for the production of tamoxifen *N*-oxide when the

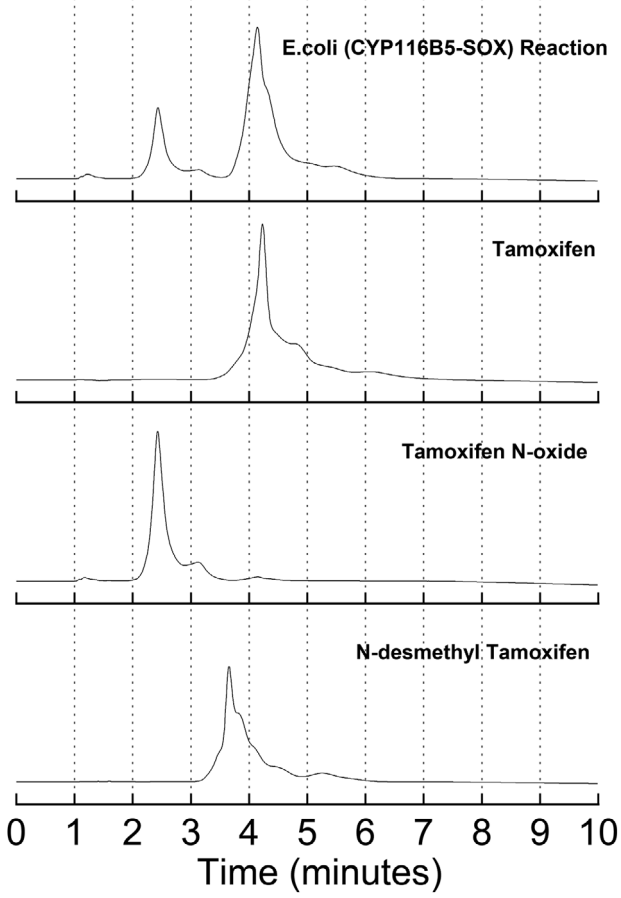

FIGURE 6 HPLC traces of tamoxifen, tamoxifen *N*-oxide and N-desmethyl tamoxifen standards, compared to the metabolites extracted with ethyl acetate from the whole cell production process using *E. coli* strain expressing CYP116B5-SOX in presence of 250 mM sarcosine and 1 mM tamoxifen.

catalysis was induced by sarcosine compared to that obtained by the direct addition of exogenous H_2O_2. The data indicate that sarcosine is an excellent driver for the catalysis of the CYP116B5-SOX in a whole cell context. We assume that the unsuitability of hydrogen peroxide as direct CYP116B5-SOX catalysis driver in whole cell context lies in the general instability of this compound, as well as in the activity of oxidative stress regulators such as catalase expressed by *E. coli*,[74,75] which result in a very low exposure of the enzyme to H_2O_2. To our knowledge, no strain of *E. coli* is capable metabolizing sarcosine and for this reason sarcosine is able to target the CYP116B5-SOX enzyme even inside the cell without being degraded by the cell endogenous metabolism.[76–78] In light of these results, we consider the SOX-based fusion enzyme system an optimal strategy to scale-up the CYP116B5 peroxygenase catalysis when a whole cell system is required.

4 | DISCUSSION

The present study is an application of the *Molecular Lego*[79] approach to obtain an in-situ generation system of H_2O_2 for the CYP116B5-

18607314, 2024, 5, Downloaded from https://analyticalsciencejournals.onlinelibrary.wiley.com/doi/10.1002/biot.202300664 by Universita Di Torino, Wiley Online Library on [14/05/2024]. See the Terms and Conditions (https://onlinelibrary.wiley.com/terms-and-conditions) on Wiley Online Library for rules of use; OA articles are governed by the applicable Creative Commons License

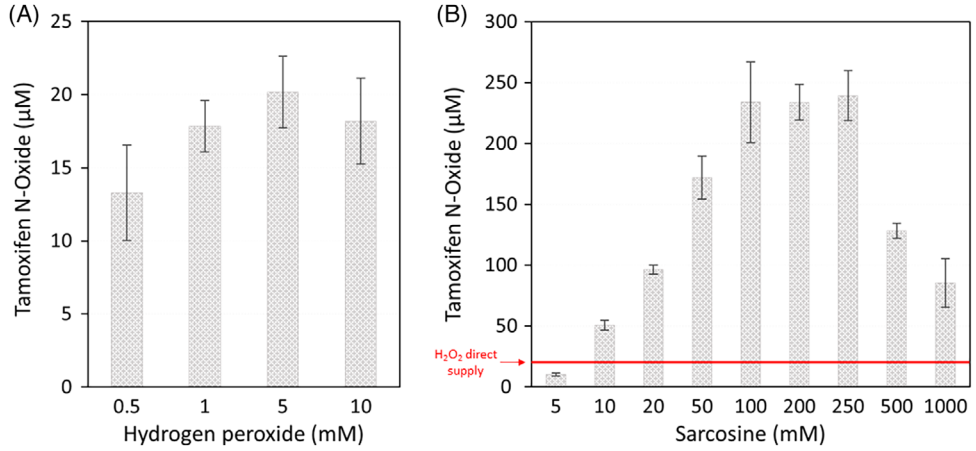

FIGURE 7 Tamoxifen *N*-oxide production exploiting *E. coli* strain expressing CYP116B5-SOX. Cell samples containing 1 mM tamoxifen were extracted with ethylacetate and analyzed by HPLC after 24 h. incubation at 30°C in presence of either increasing concentration of H_2O_2 (A) or sarcosine (B) as reaction starter. The red horizontal line shows the maximum yield of tamoxifen *N*-oxide reached by direct addition of H_2O_2.

hd peroxygenase catalysis (Figure 1). In nature, CYP116B5-hd accepts two electrons from NADPH through its FMN-binding ferridoxin reductase, that is linked to the heme domain in a unique polypeptide. Although CYP116B5 has shown to be able to convert substrates of interest for bioremediation,[21,24,25] such as drugs commonly found in wastewater,[14] the extensive use of this biocatalyst is hampered by the affordability of the native electron donor and the general instability in solution and relatively low monooxygenase activity of the natural enzyme.[23] Notably, the CYP116B5-hd peroxygenase activity has been reported to be more efficient than the full-length monooxygenase one in terms of substrates total turnover and reaction kinetics.[23,24] As the H_2O_2 direct in-bulk addition is not feasible to harness and scale-up the enzyme catalysis, several H_2O_2 supply method can be exploited, including the continuous-flow addition.[80,81] However, none of these is able to conveniently sustain the catalysis in whole cell. The protein engineering strategy by which two enzymes of different species of origin are fused to build a catalytically self-sufficient chimera, has showed remarkable results.[42–44,79,82] Moreover, the use of fusion enzyme partner(s) often enables a higher yield of protein that are difficult to be produced because of poor stability in solution.[83] In our latest work, a preliminary test carried out on cell extract of *E. coli* strain expressing the CYP116B5-SOX showed a better activity compared to CYP116B5-fl and CYP116B5-hd in the same experimental conditions.[23] Recently, SOX has been used as H_2O_2 donor partner of CYP152 peroxygenase, enabling to increase the catalytic performance of the P450.[43] As the research in the field of fusion enzymes expanded extensively in the last few years, further possible optimization of protein engineering emerged, including the modification of the sequence of the linker in terms of length and/or rigidity, as well as use other H_2O_2-generation system(s).[84,85] Interestingly, the Molecular Lego approach we pioneered, allow us to modify each module of the chimera—, that is, the linker sequence or the H_2O_2-donor domain—to further optimize the stability and activity of the P450 fusion enzyme. In light of the previous results, herein the fusion enzyme has been heterologously expressed in *E. coli*, purified and characterized in terms of domain functionalities, thermal stability and tolerance toward H_2O_2 (Figures 2, 3, and 4). CYP116B5-hd raised interest for its product specificity, being able to convert drugs into interesting compound.[21] One of the limiting aspects to the applicability of this biocatalyst is the relatively low turnover. This work of protein engineering is a promising starting point not only to obtain the fine regulation of the CYP116B5 peroxygenase activity, but also to scale up the catalysis in whole cell. In the future, this fusion enzyme strategy could be combined with the engineering of CYP116B5 active site to increase the turnover number of the enzyme, achieving additional product yield. In summary, in this work data indicate a good maturation process of the two enzymes in the fusion protein, which displayed to preserve the active folding state and the reactivity of the SOX[45,48] and CYP116B5-hd.[21,25] The folding cooperativity and the stability in solution of the two enzymes in the fusion protein have been observed during DSC experiments as well. As matter of fact, the enthalpy associated to the heme and flavin domains denaturation in the CYP116B5-SOX system is high, indicating a large amount of folded enzyme and a good homogeneity of the protein. Furthermore, the unfolding transition of the P450 domain in the artificial fusion enzyme showed a T_M increase of 3.4°C compared to the CYP116B5-fl.[21] Overall, the spectroscopy and calorimetry data indicate that the engineering strategy by which the two enzymes are linked through a poly-glycine flexible linker, resulted in the preservation of the active folding state of the two enzyme, with a increase of the stability of the heme domain.[23] The fluorescence investigation of the SOX domain reactivity revealed a relatively rapid reduction of the enzyme in presence of an excess of sarcosine, whereas the re-oxidation of SOX $FADH_2$, that is associated to the production of H_2O_2, was found to be the limiting rate step (Figure 2).[47,48] Indeed, we observed that the relatively slow re-oxidation rate of the SOX flavin is a desired process because we can achieve a controlled and continuous H_2O_2 production overtime. The CYP116B5-SOX heme leakage and loss of activity at the H_2O_2 concentration range that is accumulated by SOX activity—3–4 mM (Figure S4)—was found to be substantially neglectable in our experiments (Figure 4, table 1), indicating a great chemi-

18607314, 2024, 5, Downloaded from https://analyticalsciencejournals.onlinelibrary.wiley.com/doi/10.1002/biot.202300664 by Universita Di Torino, Wiley Online Library on [14/05/2024]. See the Terms and Conditions (https://onlinelibrary.wiley.com/terms-and-conditions) on Wiley Online Library for rules of use; OA articles are governed by the applicable Creative Commons License

cal stability of the P450 when the in-situ peroxide generation was employed.

The use of sarcosine to drive the purified CYP116B5-SOX catalysis resulted in the enhancement of the k_{cat}/K_M for pNP conversion compared to both the CYP116B5-fl (driven by NADPH), the CYP116B5-hd (H_2O_2), or CYP116B5-SOX itself when exogenous H_2O_2 was directly added in solution (Figure 5). The kinetic parameters herein registered for the pNP conversion are indeed the best ever reported for the CYP116B5.[21,23,24] In light of the latter remarkable result, we infer that by regulating the supply of H_2O_2 overtime, acting on the SOX activity, the accumulation of the peroxide in solution can be fine-tuned, limiting the oxidative damage to the heme while the P450 peroxygenase catalysis is fully sustained. We conclude that the modulation of the H_2O_2 accumulation in solution, combined to the observed high stability of the enzyme against oxidative damage and thermal denaturation, resulted in the increased catalytic performance of the CYP116B5-SOX. When tested for its bioremediation potential, the fusion enzyme showed approximately a 12-folds higher tamoxifen *N*-oxide yield compared to the direct addition of exogenous H_2O_2. In view of the outstanding results obtained by the CYP116B5-SOX system in *E. coli*, the in-situ production of H_2O_2 using sarcosine as sacrificial substrate can be considered as an optimal strategy to further characterize and scale-up the catalysis of peroxygenases P450s into whole cell systems.

AUTHOR CONTRIBUTIONS

Daniele Giuriato: conceptualization; investigation; data curation; formal analysis; visualization; writing original draft; Gianluca Catucci: conceptualization; investigation; writing; reviewing; Danilo Correddu: formal analysis; visualization; Giovanna Di Nardo: formal analysis; visualization; Gianfranco Gilardi: supervision; conceptualization; resources; supervision; writing; reviewing and editing.

CONFLICT OF INTEREST STATEMENT

The authors declare no conflict of interest.

AUTHOR INFORMATIONS

All authors' address is: Department of Life Sciences and Systems Biology, University of Torino, Via Accademia Albertina 13, 10123, Torino, Italy.

DATA AVAILABILITY STATEMENT

The data that support the findings of this study are available from the corresponding author upon reasonable request.

ORCID

Gianfranco Gilardi https://orcid.org/0000-0002-6559-276X

REFERENCES

1. Pandey, G., & Jain, R. K. (2002). Bacterial chemotaxis toward environmental pollutants: Role in bioremediation. *Applied and Environmental Microbiology*, *68*(12), 5789–5795. https://doi.org/10.1128/AEM.68.12.5789-5795.2002
2. Singh, R., Paul, D., & Jain, R. K. (2006). Biofilms: Implications in bioremediation. *Trends in Microbiology*, *14*(9), 389–397. https://doi.org/10.1016/j.tim.2006.07.001
3. aus der Beek, T., Weber, F. A., Bergmann, A., Hickmann, S., Ebert, I., Hein, A., & Küster, A. (2016). Pharmaceuticals in the environment—Global occurrences and perspectives. *Environmental Toxicology and Chemistry*, *35*(4), 823–835. https://doi.org/10.1002/etc.3339
4. Kümmerer, K. (2009). The presence of pharmaceuticals in the environment due to human use – present knowledge and future challenges. *Journal of Environmental Management*, *90*(8), 2354–2366. https://doi.org/10.1016/j.jenvman.2009.01.023
5. Ebele, A. J., Abou-Elwafa Abdallah, M., & Harrad, S. (2017). Pharmaceuticals and personal care products (PPCPs) in the freshwater aquatic environment. *Emerging Contaminants*, 3(1), 1–16. https://doi.org/10.1016/j.emcon.2016.12.004
6. Brown, K. D., Kulis, J., Thomson, B., Chapman, T. H., & Mawhinney, D. B. (2006). Occurrence of antibiotics in hospital, residential, and dairy effluent, municipal wastewater, and the Rio Grande in New Mexico. *Science of The Total Environment*, *366*(2), 772–783. https://doi.org/10.1016/j.scitotenv.2005.10.007
7. Larsson, D. G. J., de Pedro, C., & Paxeus, N. (2007). Effluent from drug manufactures contains extremely high levels of pharmaceuticals. *Journal of Hazardous Materials*, *148*(3), 751–755. https://doi.org/10.1016/j.jhazmat.2007.07.008
8. Sanderson, H., Brain, R. A., Johnson, D. J., Wilson, C. J., & Solomon, K. R. (2004). Toxicity classification and evaluation of four pharmaceuticals classes: Antibiotics, antineoplastics, cardiovascular, and sex hormones. *Toxicology*, *203*(1), 27–40. https://doi.org/10.1016/j.tox.2004.05.015
9. Wormington, A. M., De María, M., Kurita, H. G., Bisesi, J. H., Denslow, N. D., & Martyniuk, C. J. (2020). Antineoplastic agents: Environmental prevalence and adverse outcomes in aquatic organisms. *Environmental Toxicology and Chemistry*, *39*(5), 967–985. https://doi.org/10.1002/etc.4687
10. Azuma, T. (2018). Distribution of anticancer drugs in river waters and sediments of the Yodo river Basin, Japan. *Applied Sciences*, *8*(11), Article 11. https://doi.org/10.3390/app8112043
11. Franquet-Griell, H., Cornadó, D., Caixach, J., Ventura, F., & Lacorte, S. (2017). Determination of cytostatic drugs in Besòs River (NE Spain) and comparison with predicted environmental concentrations. *Environmental Science and Pollution Research*, *24*(7), 6492–6503. https://doi.org/10.1007/s11356-016-8337-y
12. Roberts, P. H., & Thomas, K. V. (2006). The occurrence of selected pharmaceuticals in wastewater effluent and surface waters of the lower Tyne catchment. *Science of The Total Environment*, *356*(1), 143–153. https://doi.org/10.1016/j.scitotenv.2005.04.031
13. Roepke, T. A., Snyder, M. J., & Cherr, G. N. (2005). Estradiol and endocrine disrupting compounds adversely affect development of sea urchin embryos at environmentally relevant concentrations. *Aquatic Toxicology*, *71*(2), 155–173. https://doi.org/10.1016/j.aquatox.2004.11.003
14. Mills, L. J., Henderson, W. M., Jayaraman, S., Gutjahr-Gobell, R. E., Zaroogian, G. E., Horowitz, D. B., & Laws, S. C. (2016). Approaches for predicting effects of unintended environmental exposure to an endocrine active pharmaceutical, tamoxifen. *Environmental Toxicology*, *31*(12), 1834–1850. https://doi.org/10.1002/tox.22184
15. Rodenas, M. C., Cabas, I., García-Alcázar, A., Meseguer, J., Mulero, V., & García-Ayala, A. (2016). Selective estrogen receptor modulators differentially alter the immune response of gilthead seabream juveniles. *Fish & Shellfish Immunology*, *52*, 189–197. https://doi.org/10.1016/j.fsi.2016.03.041
16. Di Nardo, G., & Gilardi, G. (2012). Optimization of the bacterial cytochrome P450 BM3 system for the production of human drug metabolites. *International Journal of Molecular Sciences*, *13*(12), Article 12. https://doi.org/10.3390/ijms131215901

18607314, 2024, 5, Downloaded from https://analyticalsciencejournals.onlinelibrary.wiley.com/doi/10.1002/biot.202300664 by Universita Di Torino, Wiley Online Library on [14/05/2024]. See the Terms and Conditions (https://onlinelibrary.wiley.com/terms-and-conditions) on Wiley Online Library for rules of use; OA articles are governed by the applicable Creative Commons License

17. Di Nardo, G., & Gilardi, G. (2020). Natural compounds as pharmaceuticals: The key role of cytochromes P450 reactivity. *Trends in Biochemical Sciences*, *45*(6), 511–525. https://doi.org/10.1016/j.tibs.2020.03.004
18. Whitehouse, C. J. C., Bell, S. G., & Wong, L. L. (2012). P450 BM3 (CYP102A1): Connecting the dots. *Chemical Society Reviews*, *41*(3), 1218–1260. https://doi.org/10.1039/C1CS15192D
19. Tsotsou, G. E., Sideri, A., Goyal, A., Di Nardo, G., & Gilardi, G. (2012). Identification of mutant Asp251Gly/Gln307His of Cytochrome P450 BM3 for the generation of metabolites of diclofenac, ibuprofen and tolbutamide. *Chemistry – A European Journal*, *18*(12), 3582–3588. https://doi.org/10.1002/chem.201102470
20. Caswell, J. M., O'Neill, M., Taylor, S. J., & Moody, T. S. (2013). Engineering and application of P450 monooxygenases in pharmaceutical and metabolite synthesis. *Current Opinion in Chemical Biology*, *17*(2), 271–275. https://doi.org/10.1016/j.cbpa.2013.01.028
21. Ciaramella, A., Catucci, G., Di Nardo, G., Sadeghi, S. J., & Gilardi, G. (2020). Peroxide-driven catalysis of the heme domain of A. radioresistens cytochrome P450 116B5 for sustainable aromatic rings oxidation and drug metabolites production. *New Biotechnology*, *54*, 71–79. https://doi.org/10.1016/j.nbt.2019.08.005
22. Correddu, D., Nardo, G. D., & Gilardi, G. (637477344000000000). Self-sufficient class VII cytochromes P450: From full-length structure to synthetic biology applications. *Trends in Biotechnology*, *39*(11), 1184–1207. https://doi.org/10.1016/j.tibtech.2021.01.011
23. Correddu, D., Catucci, G., Giuriato, D., Nardo, G. D., Ciaramella, A., & Gilardi, G. (2022). Catalytically self-sufficient CYP116B5: Domain switch for improved peroxygenase activity [Preprint]. Preprints. https://doi.org/10.22541/au.167101784.49533648/v1
24. Ciaramella, A., Catucci, G., Gilardi, G., & Di Nardo, G. (2019). Crystal structure of bacterial CYP116B5 heme domain: New insights on class VII P450s structural flexibility and peroxygenase activity. *International Journal of Biological Macromolecules*, *140*, 577–587. https://doi.org/10.1016/j.ijbiomac.2019.08.141
25. Minerdi, D., Sadeghi, S. J., Di Nardo, G., Rua, F., Castrignanò, S., Allegra, P., & Gilardi, G. (2015). CYP116B5: A new class VII catalytically self-sufficient cytochrome P 450 from Acinetobacter radioresistens that enables growth on alkanes. *Molecular Microbiology*, *95*(3), 539–554. https://doi.org/10.1111/mmi.12883
26. Famulari, A., Correddu, D., Di Nardo, G., Gilardi, G., Chiesa, M., & García-Rubio, I. (2022). EPR characterization of the heme domain of a self-sufficient cytochrome P450 (CYP116B5). *Journal of Inorganic Biochemistry*, *231*, 111785. https://doi.org/10.1016/j.jinorgbio.2022.111785
27. Famulari, A., Correddu, D., Nardo, G. D., Gilardi, G., Chiesa, M., & García-Rubio, I. (2022). CYP116B5hd, a self-sufficient P450 cytochrome: A dataset of its electronic and geometrical properties, *42*, 108195. https://doi.org/10.1016/j.dib.2022.108195
28. Kinner, A., Rosenthal, K., & Lütz, S. (2021). Identification and expression of new unspecific peroxygenases – Recent advances, challenges and opportunities. *Frontiers in Bioengineering and Biotechnology*, *9*, 705630. https://www.frontiersin.org/articles/10.3389/fbioe.2021.705630
29. Grogan, G. (2021). Hemoprotein catalyzed oxygenations: P450s, UPOs, and progress toward scalable reactions. *JACS Au*, *1*(9), 1312–1329. https://doi.org/10.1021/jacsau.1c00251
30. Wang, Y., Lan, D., Durrani, R., & Hollmann, F. (2017). Peroxygenases en route to becoming dream catalysts. What are the opportunities and challenges? *Current Opinion in Chemical Biology*, *37*, 1–9. https://doi.org/10.1016/j.cbpa.2016.10.007
31. Urlacher, V. B., & Girhard, M. (2019). Cytochrome P450 monooxygenases in biotechnology and synthetic biology biotechnology and synthetic biology. *Trends in Biotechnology*, *37*(8), 882–897. https://doi.org/10.1016/j.tibtech.2019.01.001
32. Hrycay, E. G., & Bandiera, S. M. (2015). Monooxygenase, Peroxidase and Peroxygenase Properties and Reaction Mechanisms of Cytochrome P450 Enzymes. In E. G. Hrycay, & S. M. Bandiera (Eds.), *Monooxygenase, Peroxidase and Peroxygenase Properties and Mechanisms of Cytochrome P450* (pp. 1–61). Springer International Publishing. https://doi.org/10.1007/978-3-319-16009-2_1
33. Hobisch, M., Holtmann, D., Gomez de Santos, P., Alcalde, M., Hollmann, F., & Kara, S. (2021). Recent developments in the use of peroxygenases – Exploring their high potential in selective oxyfunctionalisations. *Biotechnology Advances*, *51*, 107615. https://doi.org/10.1016/j.biotechadv.2020.107615
34. Linde, D., Olmedo, A., González-Benjumea, A., Estévez, M., Renau-Mínguez, C., Carro, J., Fernández-Fueyo, E., Gutiérrez, A., & Martínez, A. T. (2020). Two new unspecific peroxygenases from heterologous expression of fungal genes in Escherichia coli. *Applied and Environmental Microbiology*, *86*(7), e02899–e02919. https://doi.org/10.1128/AEM.02899-19
35. Bernhardt, R., & Urlacher, V. B. (2014). Cytochromes P450 as promising catalysts for biotechnological application: Chances and limitations. *Applied Microbiology and Biotechnology*, *98*(14), 6185–6203. https://doi.org/10.1007/s00253-014-5767-7
36. Schmitz, F., Koschorreck, K., Hollmann, F., & Urlacher, V. B. (2023). Aromatic hydroxylation of substituted benzenes by an unspecific peroxygenase from Aspergillus brasiliensis. *Reaction Chemistry & Engineering*, *8*(9), 2177–2186. https://doi.org/10.1039/D3RE00209H
37. Molina-Espeja, P., Garcia-Ruiz, E., Gonzalez-Perez, D., Ullrich, R., Hofrichter, M., & Alcalde, M. (2014). Directed evolution of unspecific peroxygenase from Agrocybe aegerita. *Applied and Environmental Microbiology*, *80*(11), 3496–3507. https://doi.org/10.1128/AEM.00490-14
38. Molina-Espeja, P., Ma, S., Mate, D. M., Ludwig, R., & Alcalde, M. (2015). Tandem-yeast expression system for engineering and producing unspecific peroxygenase. *Enzyme and Microbial Technology*, *73–74*, 29–33. https://doi.org/10.1016/j.enzmictec.2015.03.004
39. Correddu, D., Aly, S. H., Nardo, G. D., Catucci, G., Prandi, C., Blangetti, M., Bellomo, C., Bonometti, E., Viscardi, G., & Gilardi, G. (2022). Enhanced and specific epoxidation activity of P450 BM3 mutants for the production of high value terpene derivatives. *RSC Advances*, *12*(52), 33964–33969. https://doi.org/10.1039/D2RA06029A
40. Ezraty, B., Gennaris, A., Barras, F., & Collet, J. F. (2017). Oxidative stress, protein damage and repair in bacteria. *Nature Reviews Microbiology*, *15*(7), Article 7. https://doi.org/10.1038/nrmicro.2017.26
41. Catucci, G., Ciaramella, A., Di Nardo, G., Zhang, C., Castrignanò, S., & Gilardi, G. (2022). Molecular lego of human cytochrome P450: The key role of heme domain flexibility for the activity of the chimeric proteins. *International Journal of Molecular Sciences*, *23*(7), Article 7. https://doi.org/10.3390/ijms23073618
42. Sadeghi, S. J., & Gilardi, G. (2013). Chimeric P450 enzymes: Activity of artificial redox fusions driven by different reductases for biotechnological applications. *Biotechnology and Applied Biochemistry*, *60*(1), 102–110. https://doi.org/10.1002/bab.1086
43. Giuriato, D., Correddu, D., Catucci, G., Di Nardo, G., Bolchi, C., Pallavicini, M., & Gilardi, G. (2022). Design of a H 2 O 2 -generating P450 SPα fusion protein for high yield fatty acid conversion. *Protein Science*, 31(12), e4501. https://doi.org/10.1002/pro.4501
44. Degregorio, D., D'Avino, S., Castrignanò, S., Di Nardo, G., Sadeghi, S. J., Catucci, G., & Gilardi, G. (2017). Human cytochrome P450 3A4 as a biocatalyst: Effects of the engineered linker in modulation of coupling efficiency in 3A4-BMR chimeras. *Frontiers in Pharmacology*, *8*, 121. https://www.frontiersin.org/articles/10.3389/fphar.2017.00121
45. Trickey, P., Wagner, M. A., Jorns, M. S., & Mathews, F. S. (1999). Monomeric sarcosine oxidase: Structure of a covalently flavinylated amine oxidizing enzyme. *Structure*, *7*(3), 331–345. https://doi.org/10.1016/S0969-2126(99)80043-4
46. Wagner, M. A., Khanna, P., & Jorns, M. S. (1999). Structure of the flavocoenzyme of two homologous amine oxidases: Monomeric sar-

18607314, 2024, 5, Downloaded from https://analyticalsciencejournals.onlinelibrary.wiley.com/doi/10.1002/biot.202300664 by Universita Di Torino, Wiley Online Library on [14/05/2024]. See the Terms and Conditions (https://onlinelibrary.wiley.com/terms-and-conditions) on Wiley Online Library for rules of use; OA articles are governed by the applicable Creative Commons License

cosine oxidase and N -methyltryptophan oxidase. *Biochemistry*, *38*(17), 5588–5595. https://doi.org/10.1021/bi982955o

47. Wagner, M. A., Trickey, P., Chen, Z. W., Mathews, F. S., & Jorns, M. S. (2000). Monomeric sarcosine oxidase: 1. Flavin reactivity and active site binding determinants. *Biochemistry*, *39*(30), 8813–8824. https://doi.org/10.1021/bi000349z
48. Wagner, M. A., & Jorns, M. S. (2000). Monomeric Sarcosine Oxidase: 2. Kinetic studies with sarcosine, alternate substrates, and a substrate analogue. *Biochemistry*, *39*(30), 8825–8829. https://doi.org/10.1021/bi000350y
49. Chlumsky, L. J., Zhang, L., & Jorns, M. S. (1995). Sequence analysis of sarcosine oxidase and nearby genes reveals homologies with key enzymes of folate one-carbon metabolism. *Journal of Biological Chemistry*, *270*(31), 18252–18259. https://doi.org/10.1074/jbc.270.31.18252
50. Zhao, G., & Jorns, M. S. (2006). Spectral and kinetic characterization of the Michaelis charge transfer complex in monomeric sarcosine oxidase. *Biochemistry*, *45*(19), 5985–5992. https://doi.org/10.1021/bi0600852
51. Gao, C., Catucci, G., Castrignanò, S., Gilardi, G., & Sadeghi, S. J. (2017). Inactivation mechanism of N61S mutant of human FMO3 towards trimethylamine. *Scientific Reports*, *7*(1), 14668. https://doi.org/10.1038/s41598-017-15224-9
52. Di Nardo, G., Cimicata, G., Baravalle, R., Dell'Angelo, V., Ciaramella, A., Catucci, G., Ugliengo, P., & Gilardi, G. (2018). Working at the membrane interface: Ligand-induced changes in dynamic conformation and oligomeric structure in human aromatase. *Biotechnology and Applied Biochemistry*, *65*(1), 46–53. https://doi.org/10.1002/bab.1613
53. Catucci, G., Aramini, D., Sadeghi, S. J., & Gilardi, G. (2020). Ligand stabilization and effect on unfolding by polymorphism in human flavin-containing monooxygenase 3. *International Journal of Biological Macromolecules*, *162*, 1484–1493. https://doi.org/10.1016/j.ijbiomac.2020.08.032
54. Li, Q., Sritharathikhun, P., & Motomizu, S. (2007). Development of novel reagent for Hantzsch reaction for the determination of formaldehyde by spectrophotometry and fluorometry. *Analytical Sciences: The International Journal of the Japan Society for Analytical Chemistry*, *23*(4), 413–417. https://doi.org/10.2116/analsci.23.413
55. Kadnikova, E. N., & Kostić, N. M. (2002). Oxidation of ABTS by hydrogen peroxide catalyzed by horseradish peroxidase encapsulated into sol–gel glass.: Effects of glass matrix on reactivity. *Journal of Molecular Catalysis B: Enzymatic*, *18*(1), 39–48. https://doi.org/10.1016/S1381-1177(02)00057-7
56. Vuong, T. V., Vesterinen, A.-H., Foumani, M., Juvonen, M., Seppälä, J., Tenkanen, M., & Master, E. R. (2013). Xylo- and cello-oligosaccharide oxidation by gluco-oligosaccharide oxidase from Sarocladium strictumand variants with reduced substrate inhibition. *Biotechnology for Biofuels*, *6*(1), 148. https://doi.org/10.1186/1754-6834-6-148
57. Zeller, H. D., Hille, R., & Jorns, M. S. (1989). Bacterial sarcosine oxidase: Identification of novel substrates and a biradical reaction intermediate. *Biochemistry*, *28*(12), 5145–5154. https://doi.org/10.1021/bi00438a035
58. Nelson, D. R. (2005). Cytochrome P450: Structure, Mechanism, and Biochemistry, 3rd ed Edited by Paul R. Ortiz de Montellano (University of California, San Francisco). Kluwer Academic/Plenum Publishers: New York. 2005. xx + 690 pp. $149.00. ISBN 0-306-48324-6., 3rd ed Edited by Paul R. Ortiz de Montellano (University of California, San Francisco). Kluwer Academic/Plenum Publishers: New York. 2005. xx + 690 pp. $149.00. ISBN 0-306-48324-6. *Journal of the American Chemical Society*, *127*(34), 12147–12148. https://doi.org/10.1021/ja041050x
59. Omura, T., & Sato, R. (1964). The carbon monoxide-binding pigment of liver microsomes: I. Evidence for its hemoprotein nature. *Journal of Biological Chemistry*, *239*(7), 2370–2378. https://doi.org/10.1016/S0021-9258(20)82244-3
60. Tong, Y., Xin, Y., Yang, H., Zhang, L., & Wang, W. (2014). Efficient improvement on stability of sarcosine oxidase via poly-lysine modification on enzyme surface. *International Journal of Biological Macromolecules*, *67*, 140–146. https://doi.org/10.1016/j.ijbiomac.2014.03.015
61. Xin, Y., Zheng, M., Wang, Q., Lu, L., Zhang, L., Tong, Y., & Wang, W. (2016). Structural and catalytic alteration of sarcosine oxidase through reconstruction with coenzyme-like ligands. *Journal of Molecular Catalysis B: Enzymatic*, *133*, S250–S258. https://doi.org/10.1016/j.molcatb.2017.01.011
62. Albertolle, M. E., Kim, D., Nagy, L. D., Yun, C.-H., Pozzi, A., Savas, Ü., Johnson, E. F., & Guengerich, F. P. (2017). Heme–thiolate sulfenylation of human cytochrome P450 4A11 functions as a redox switch for catalytic inhibition. *Journal of Biological Chemistry*, *292*(27), 11230–11242. https://doi.org/10.1074/jbc.M117.792200
63. Matthews, S., Tee, K. L., Rattray, N. J., McLean, K. J., Leys, D., Parker, D. A., Blankley, R. T., & Munro, A. W. (2017). Production of alkenes and novel secondary products by P450 Ole T JE using novel H 2 O 2 -generating fusion protein systems. *FEBS Letters*, *591*(5), 737–750. https://doi.org/10.1002/1873-3468.12581
64. Lee, Y., Sathesh-Prabu, C., Kwak, G. H., Bang, I., Jung, H. W., Kim, D., & Lee, S. K. (2022). Enhanced production of nonanedioic acid from nonanoic acid by engineered Escherichia coli. *Biotechnology Journal*, *17*(3), e2000416. Scopus. https://doi.org/10.1002/biot.202000416
65. Opdensteinen, P., & Buyel, J. F. (2022). Reducing water uptake into BY-2 cells by systematically optimizing the cultivation parameters increases product yields achieved by transient expression in plant cell packs. *Biotechnology Journal*, *17*(10), e2200134. Scopus. https://doi.org/10.1002/biot.202200134
66. Yoshino, T., Mao, Y., Maeda, Y., Negishi, R., Murata, S., Moriya, S., Shimada, H., Arakaki, A., Kobayashi, K., Hagiwara, Y., Okamoto, K., & Tanaka, T. (2022). Single-cell genotyping of phytoplankton from ocean water by gel-based cell manipulation. *Biotechnology Journal*, 17(6). Scopus. https://doi.org/10.1002/biot.202100633
67. Yu, C., Zhong, H., Yang, X., Li, G., Wu, Z., & Yang, H. (2022). Establishment of a pig CRISPR/Cas9 knockout library for functional gene screening in pig cells. *Biotechnology Journal*, 17(7). Scopus. https://doi.org/10.1002/biot.202100408
68. Carniel, A., Santos, A. G., Chinelatto, L. S., Castro, A. M., & Coelho, M. A. Z. (2023). Biotransformation of ethylene glycol to glycolic acid by Yarrowia lipolytica: A route for poly(ethylene terephthalate) (PET) upcycling. *Biotechnology Journal*, 18(6). Scopus. https://doi.org/10.1002/biot.202200521
69. Janssen, L., Sadowski, G., & Brandenbusch, C. (2023). Continuous phase separation of stable emulsions from biphasic whole-cell biocatalysis by catastrophic phase inversion. *Biotechnology Journal*, 18(6). Scopus. https://doi.org/10.1002/biot.202200489
70. Liu, Q., Li, Y., Hou, W., Zhang, B., & Bao, J. (2023). Cellulase mediated stress triggers the mutations of oleaginous yeast Trichosporon cutaneum with super-large spindle morphology and high lipid accumulation. *Biotechnology Journal*, *18*(8), e2300091. Scopus. https://doi.org/10.1002/biot.202300091
71. Wang, M., Wang, M., Li, W., Liu, Y., & Qiu, F. (2023). Single-cell detection of DMSO promoted HL-60 differentiation toward granulocyte based on DC-iDEP for medicine screening. *Biotechnology Journal*, *18*(12), e2300073. Scopus. https://doi.org/10.1002/biot.202300073
72. Qiao, Y., Ma, W., Zhang, S., Guo, F., Liu, K., Jiang, Y., Wang, Y., Xin, F., Zhang, W., & Jiang, M. (2023). Artificial multi-enzyme cascades and whole-cell transformation for bioconversion of C1 compounds: Advances, challenge and perspectives. *Synthetic and Systems Biotechnology*, *8*(4), 578–583. https://doi.org/10.1016/j.synbio.2023.08.008
73. Zhang, H., Zhao, A., Qu, L., Xiong, W., Alam, M. A., Miao, J., Wang, W., Xu, J., & Lv, Y. (2023). Engineering an efficient whole-cell catalyst for d -allulose production from glycerol. *Biotechnology Journal*, *18*(7), e2200600. Scopus. https://doi.org/10.1002/biot.202200600

18607314, 2024, 5, Downloaded from https://analyticalsciencejournals.onlinelibrary.wiley.com/doi/10.1002/biot.202300664 by Universita Di Torino, Wiley Online Library on [14/05/2024]. See the Terms and Conditions (https://onlinelibrary.wiley.com/terms-and-conditions) on Wiley Online Library for rules of use; OA articles are governed by the applicable Creative Commons License

74. Chiang, S. M., & Schellhorn, H. E. (2012). Regulators of oxidative stress response genes in Escherichia coli and their functional conservation in bacteria. *Archives of Biochemistry and Biophysics*, *525*(2), 161–169. https://doi.org/10.1016/j.abb.2012.02.007
75. Hansberg, W. (2022). Monofunctional heme-catalases. *Antioxidants (Basel, Switzerland)*, *11*(11), 2173. https://doi.org/10.3390/antiox11112173
76. Kanehisa, M. (2019). Toward understanding the origin and evolution of cellular organisms. *Protein Science*, *28*(11), 1947–1951. https://doi.org/10.1002/pro.3715
77. Kanehisa, M., & Goto, S. (2000). KEGG: Kyoto encyclopedia of genes and genomes. *Nucleic Acids Research*, *28*(1), 27–30. https://doi.org/10.1093/nar/28.1.27
78. Kanehisa, M., Furumichi, M., Sato, Y., Kawashima, M., & Ishiguro-Watanabe, M. (2023). KEGG for taxonomy-based analysis of pathways and genomes. *Nucleic Acids Research*, *51*(D1), D587–D592. https://doi.org/10.1093/nar/gkac963
79. Gilardi, G., Meharenna, Y. T., Tsotsou, G. E., Sadeghi, S. J., Fairhead, M., & Giannini, S. (2002). Molecular Lego: Design of molecular assemblies of P450 enzymes for nanobiotechnology. *Biosensors & Bioelectronics*, *17*(1–2), 133–145. https://doi.org/10.1016/s0956-5663(01)00286-x
80. Britton, J., Majumdar, S., & Weiss, G. A. (2018). Continuous flow biocatalysis. *Chemical Society Reviews*, *47*(15), 5891–5918. https://doi.org/10.1039/c7cs00906b
81. Marinho, H. S., Cyrne, L., Cadenas, E., & Antunes, F. (2013). Chapter Ten – H^2O^2 Delivery to Cells: Steady-State Versus Bolus Addition. In E. Cadenas & L. Packer (Eds.), *Methods in Enzymology* (Vol. 526, pp. 159–173). Academic Press. https://doi.org/10.1016/B978-0-12-405883-5.00010-7
82. Paul, C. E., Churakova, E., Maurits, E., Girhard, M., Urlacher, V. B., & Hollmann, F. (2014). In situ formation of H^2O^2 for P450 peroxygenases. *Bioorganic & Medicinal Chemistry*, *22*(20), 5692–5696. https://doi.org/10.1016/j.bmc.2014.05.074
83. Lyons-Abbott, S., Abramov, A., Chan, C., Deer, J. R., Fu, G., Hassouneh, W., Koch, T., Misquith, A., O'Neill, J., Simon, S. A., Wolf, A., Yeh, R., & Vernet, E. (2024). Choice of fusion proteins, expression host, and analytics solves difficult-to-produce protein challenges in discovery research. *Biotechnology Journal*, *19*(1), 2300162. https://doi.org/10.1002/biot.202300162
84. Monterrey, D. T., Ayuso-Fernández, I., Oroz-Guinea, I., & García-Junceda, E. (2022). Design and biocatalytic applications of genetically fused multifunctional enzymes. *Biotechnology Advances*, *60*, 108016. https://doi.org/10.1016/j.biotechadv.2022.108016
85. Ma, Y., Zhang, N., Vernet, G., & Kara, S. (2022). Design of fusion enzymes for biocatalytic applications in aqueous and non-aqueous media. *Frontiers in Bioengineering and Biotechnology*, *10*, 944226. https://www.frontiersin.org/articles/10.3389/fbioe.2022.944226

SUPPORTING INFORMATION

Additional supporting information can be found online in the Supporting Information section at the end of this article.

How to cite this article: Giuriato, D., Catucci, G., Correddu, D., Nardo, G. D., & Gilardi, G. (2024). CYP116B5-SOX: An artificial peroxygenase for drug metabolites production and bioremediation. *Biotechnology Journal*, *19*, e2300664. https://doi.org/10.1002/biot.202300664

18607314, 2024, 5, Downloaded from https://analyticalsciencejournals.onlinelibrary.wiley.com/doi/10.1002/biot.202300664 by Universita Di Torino, Wiley Online Library on [14/05/2024]. See the Terms and Conditions (https://onlinelibrary.wiley.com/terms-and-conditions) on Wiley Online Library for rules of use; OA articles are governed by the applicable Creative Commons License